Thermodynamic control of quantum defects on single-walled carbon nanotubes

Yutaka Maeda,[a*] Hiyori Murakoshi,[a] Haruto Tambo,[a] Pei Zhao,[b] Kiyonori Kuroda,[a] Michio Yamada,[a] Xiang Zhao,[c] Shigeru Nagase,[d] Masahiro Ehara[b*]

[a] Department of Chemistry, Tokyo Gakugei University, Tokyo 184-8501, Japan

[b] Research Center for Computational Science, Institute for Molecular Science, Okazaki, 444-8585, Japan

[c] Institute for Chemical Physics & Department of Chemistry, School of Science, State Key Laboratory of Electrical Insulation and Power Equipment, Xi'an Jiaotong University, Xi'an 710049, China

[d] Fukui Institute for Fundamental Chemistry (FIFC), Kyoto University, Sakyou-ku, Kyoto 606-8103, Japan

Corresponding author's e-mail: ymaeda@u-gakugei.ac.jp (YM); ehara@ims.ac.jp (ME)

Table of Contents

Experimental Section

Table S6. Relative energies (in kcal/mol) of H-SWNT-CH(CH_3)CH=CHCH$_3$ after the rearrangement of SWNT-($C_3H_4Me_2$) calculated by DFT with B3LYP/6-31G* using 1-unit cell (with respect to the most stable isomer of SWNT-($C_3H_4Me_2$) in Table 1). Calculated absorption wavelengths of H-SWNT-CH(CH_3)CH=CHCH$_3$ using TD-DFT with B3LYP/3-21G using 1-unit cell.

Table S7. Total energies (in a.u.) of functionalized (6,5) SWNTs calculated by DFT with B3LYP/6-31G* using 1-unit cell.

Table S8. Relative energies of functionalized SWNTs calculated by B3LYP, M06-2X, and ωB97XD with the 6-31G* basis sets.

Experimental Section

EXPERIMENTAL SECTION

General Information. The (6,5)-enriched SWNTs (SG 65i), used in this work, were purchased from Sigma-Aldrich. Reagent-grade dibromoalkanes were purchased from commercial suppliers. 2,4-dibromo-2-methylpentane (**1d**) and 1,3-dibromo-1,3-diphenylpropane (**1e**) were synthesized according to literature procedures in 26 and 62% yields, respectively.[1,2] Optical absorption spectra were recorded by using a spectrophotometer (V-670; Jasco Corp.). Raman spectra were measured under excitation at 514.5 and 633 nm, by using a spectrophotometer (LabRAM HR-800; Horiba Ltd.). Raman spectra were normalized relative to the G band. Photoluminescence spectra were obtained by using a spectrophotometer equipped with a 450-W lamp and a Symphony-II CCD detector (Nanolog; Horiba Ltd.). The excitation and emission wavelengths were varied from 500-1000 nm and 827-1600 nm, respectively, in 1 nm steps. The excitation and emission slit widths were 10 nm. The PL intensity was corrected to the data correction time of each sample. For absorption and PL measurements, the samples were dispersed in D_2O containing 1 wt% sodium dodecylbenzene sulfate (SDBS) by ultrasound irradiation in a bath sonicator (B2510J-MT ultrasonic cleaner; Branson) and centrifuged at 140000 *g* for 1 h in a high-speed centrifuge equipped with a P70AT2 angle rotor (CP80β; Hitachi Koki Co., Ltd.). To adjust the absorption intensity at ~775 nm, an adequate dose of D_2O solution containing SDBS was added to the dispersion depending on the concentration. After sonication, the resulting suspension was centrifuged for 1 h at 140000 g. Thermal treatment of the samples was performed at a heating rate of 10°C/min and a nitrogen flow rate of 50 mL/min (TG-50A; Shimadzu Corp.). The samples were held for 30 min at 100°C for drying. Scanning electron microscopy (SEM) was conducted using a field emission electron microscope (1.5 kV accelerating voltage, 10 μA beam current, SU8020; Hitachi Ltd.). The relative E_{11} absorption peak intensity is used as an index for the degree of functionalization of SWNTs, and is defined by the relative peak intensity, [E_{11} absorption intensity of functionalized SWNTs/intensity of local minimum near 775 nm of functionalized SWNTs]/[E_{11} absorption intensity of SWNTs/intensity of local minimum near 775 nm of SWNTs].

Computational details.

A single unit of pristine (6,5) SWNT passivated with hydrogen at the terminals was first utilized as the computational model. Functionalized SWNT-(C_3H_6), SWNT-(C_3H_5Me), SWNT-(*cis*-$C_3H_4Me_2$), SWNT-(*trans*-$C_3H_4Me_2$), SWNT-(C_4H_8), SWNT-(C_4H_7Me), SWNT-(*cis*-$C_4H_6Me_2$), and SWNT-(*trans*-$C_4H_6Me_2$) were calculated at the *ortho* positions in three different directions (L_{-33}, L_{87}, L_{27}), as shown in Figure 3. The ground states of these derivatives were optimized by DFT using the B3LYP functional with 6-31G*.[3] The TD-DFT calculations of the vertical transition energies and the optimization of excited states were performed at the B3LYP/3-21G level of theory.

The spin density on the *ortho* positions of the *n*-butylated (6,5) SWNT radical was obtained using models consisting of 1, 2, and 3-unit cells at the UB3LYP/3-21G level of theory. All DFT calculations were conducted using the Gaussian 09 suite of programs version E.01.[4]

Confinement and methodology errors were considered to evaluate emission energies of *ortho* adducts in SWNT-(C_3H_6) and SWNT-(*cis*-$C_3H_4Me_2$). The following correction formula has been utilized to estimate the emission energies of functionalized (6,5) SWNTs at infinite length $E_{11}*(\infty)$, which was proposed by Htoon and co-workers:[5]

$E_{11}*(\infty) = -0.59(E_{11}-E_{11}*) + 1.25$

where E_{11} and $E_{11}*$ represent emission energies of the pristine SWNT and each functionalized SWNT, respectively. The emission energies were calculated using 3-unit cells at the level of CAM-B3LYP/STO-3G.[6]

Typical procedure of reductive alkylation:

Naphthalene (152 mg, 1.19 mmol) and sodium (77.8 mg, 3.38 mmol) were placed in a heat-dried three-necked round-bottomed flask under argon. Anhydrous tetrahydrofuran (50 mL) was then added to the flask and the contents were stirred for 1.5 h. A portion (5.0 mg) of SWNTs was placed in a second heat-dried three-necked round-bottom flask under argon and the sodium naphthalenide solution was added to the SWNTs, and the mixture was then sonicated for 1 h. Dibromoalkane (1.43 mmol) was subsequently added to the mixture, which was sonicated for 30 min. After the addition of dry ethanol (15 mL), the resulting suspended black solid was collected by filtration using a membrane filter (PTFE, 1.0 μm) and washed with tetrahydrofuran, methanol, and distilled water by the dispersion/filtration process.

2-methyl-2,4-dibromopnetane (1d)[1]

2-methylpentane-2,4-diol (77.8 mmol, 9.2 g) was dissolved in dichloromethane (100 mL) in a dry flask under Ar atmosphere. The solution was cooled to -15°C in a NaCl-ice bath, and phosphorus tribromide (315.8 mmol, 85.5 g) was added dropwise with stirring. The mixture was stirred for 4 hours at room temperature. Water (100 mL) was added and the product extracted with dichloromethane (20 mL x 3) was washed with cold water (20 mL x 5). The organic layer was dried over anhydrous sodium sulfate. It was purified by distillation and **1d** was corrected at 47-48°C / 4 mmHg as colorless liquid. (4.9 g, 20.2 mmol, 26%) ^{1}H NMR (400 MHz, $CDCl_3$) δ = 1.81 (d, J = 6.8 Hz, 3H), 1.83 (s, 3H), 1.87 (s, *3*H), 2.43 (dd, J = 16.0, 4.1 Hz, 1H), 2.51 (dd, J = 16.0, 6.8 Hz, 1H), 4.40 (ddq, J = 6.8, 6.8, 4.1 Hz, 1H). ^{13}C NMR (100 MHz, $CDCl_3$) δ = 28.6, 33.6, 35.9, 46.4, 57.6, 66.1.

1,3-dibromo-1,3-diphenylpropane (1e)[2]

Benzaldehyde (6.0 mmol, 0.64 g) and styrene (6.0 mmol, 0.62 g) were dissolved in dichloromethane (40 mL) in a dry flask under Ar atmosphere. The solution was cooled to -40°C in a low temperature thermostated bath. Boron tribromide (6.4 mmol, 6.4 mL of a 1 M dichloromethane solution) was added via a syringe. The mixture was stirred for 2 hours at -40˚C and then for 2hours at room temperature. Water (40 mL) was added and the product extracted with dichloromethane (10 mL x 3). The combined organic layer was dried over anhydrous magnesium sulfate and the product isolated by flash column chromatography (silica gel, hexane) to yield 1.3 g (3.7 mmol, 62%) of **1e**. ^{1}H NMR (400 MHz, $CDCl_3$) δ = 2.88-2.96 (m, 1.5 H), 3.21 (dt, J = 14.6, 7.4 Hx, 0.5H), 4.86 (t, J = 6.9 Hz, 1H), 5.18 (t, J = 6.9 Hz, 1H), 7.29-7.39 (m, 10H). ^{13}C NMR (100 MHz, $CDCl_3$) δ = 49.3, 49.4, 52.0, 53.1, 127.6, 127.6, 128.9, 129.0, 129.1, 140.5, 141.1.

References

1. J. D. Bartleson, R. E. Burk and H. P. Lankelma, *J. Am. Chem. Soc.* 1946, **46**, 2513.
2. G. W. Kabalka, Z. Wu, Y. Ju, M.-L. Yao, *J. Org. Chem.* 2005, **70**, 10285.
3. A. D. Becke, *J. Chem. Phys.*, 1993, **98**, 5648-5652.
4. M. J. Frisch, G. W. Trucks, H. B. Schlegel, G. E. Scuseria, M. A. Robb, J. R. Cheeseman, G. Scalmani, V. Barone, B. Mennucci, G. A. Petersson, H. Nakatsuji, M. Caricato, X. Li, H. P. Hratchian, A. F. Izmaylov, J. Bloino, G. Zheng, J. L. Sonnenberg, M. Hada, M. Ehara, K. Toyota, R. Fukuda, J. Hasegawa, M. Ishida, T. Nakajima, Y. Honda, O. Kitao, H. Nakai, T. Vreven, J. Montgomery, J. A., J. E. Peralta, F. Ogliaro, M. Bearpark, J. J. Heyd, E. Brothers, K. N. Kudin, V. N. Staroverov, R. Kobayashi, J. Normand, K. Raghavachari, A. Rendell, J. C. Burant, S. S. Iyengar, J. Tomasi, M. Cossi, N. Rega, J. M. Millam, M. Klene, J. E. Knox, J. B. Cross, V. Bakken, C. Adamo, J. Jaramillo, R. Gomperts, R. E. Stratmann, O. Yazyev, A. J. Austin, R. Cammi, C. Pomelli, J. W. Ochterski, R. L. Martin, K. Morokuma, V. G. Zakrzewski, G. A. Voth, P. Salvador, J. J. Dannenberg, S. Dapprich, A. D. Daniels, Ö. Farkas, J. B. Foresman, J. V. Ortiz, J. Cioslowski and D. J. Fox, *Gaussian 09, Revision E.01*, Gaussian, Inc., Wallingford CT. **2013**.
5. B. J. Gifford, A. E. Sifain, H. Htoon, S. K. Doorn, S. Kilina and S. Tretiak, *J. Phys. Chem. Lett.*, 2018, **9**, 2460-2468.
6. T. Yanai and D. P. Tew, *Chem. Phys. Lett.*, 2004, **393**, 51-57.

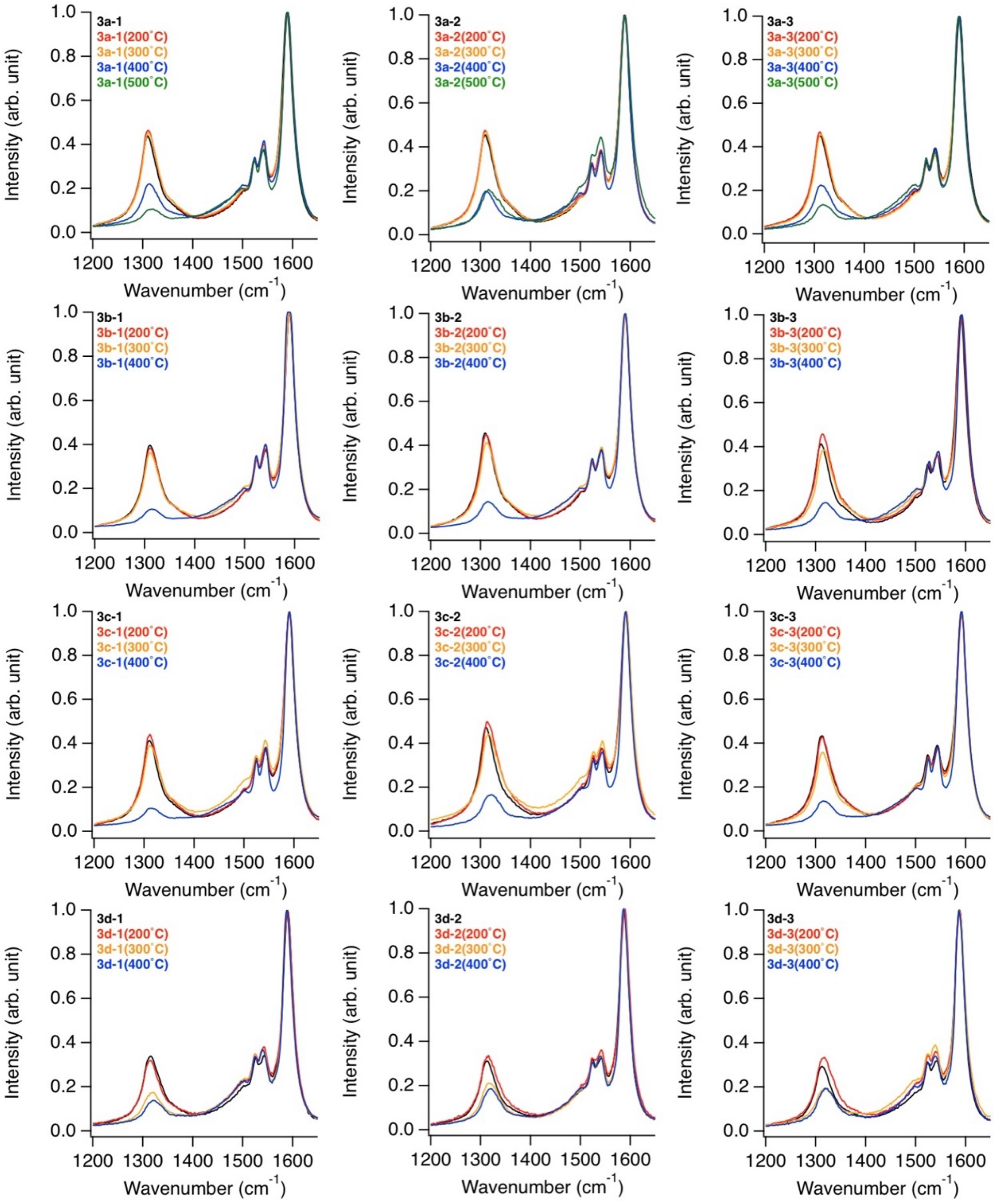

Figure S1. Raman spectra (514.5 nm excitation) of functionalized SWNTs (**3a-3d**) before and after thermal treatment.

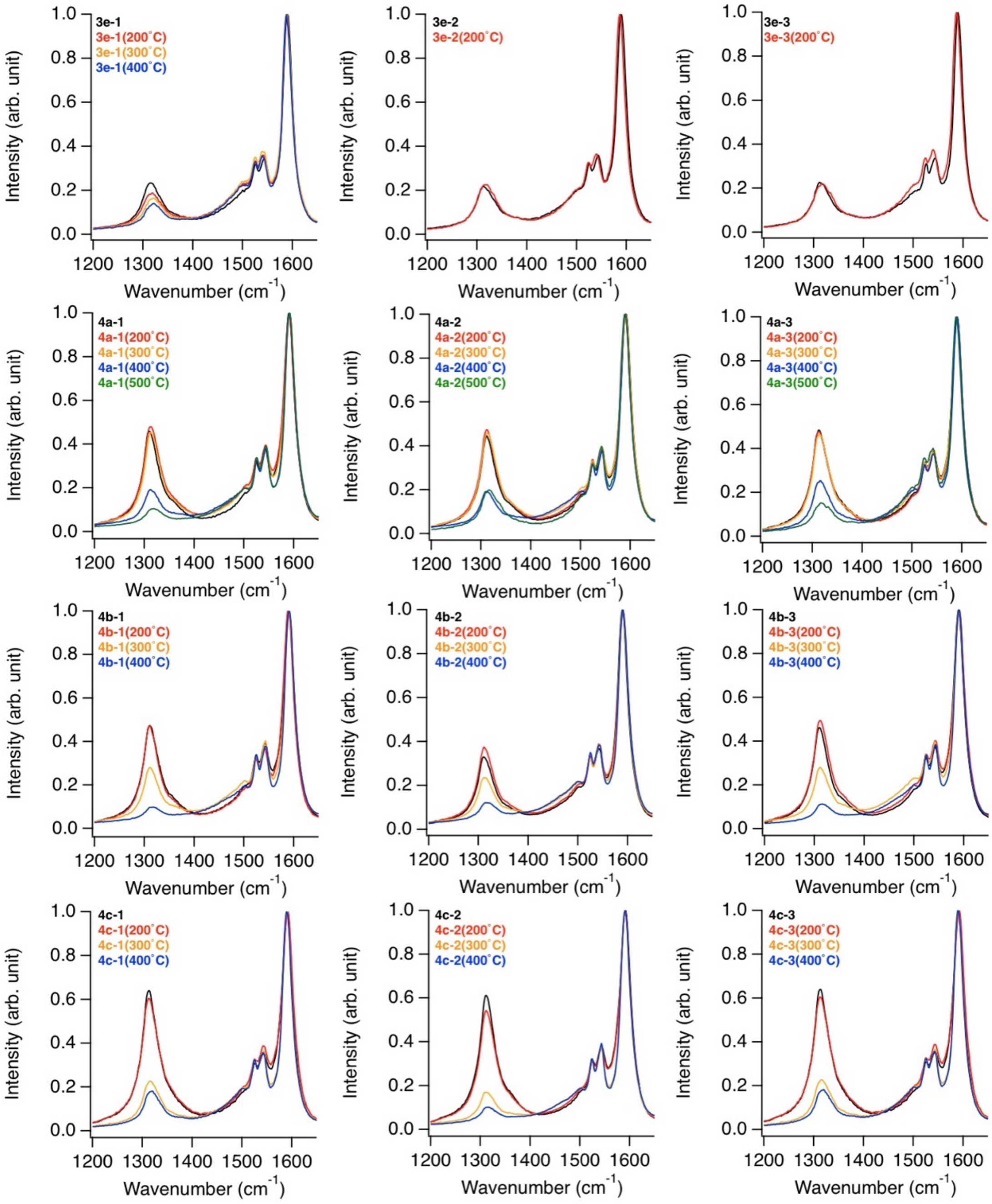

Figure S2. Raman spectra (514.5 nm excitation) of functionalized SWNTs (**3e**, **4a**-**4c**) before and after thermal treatment.

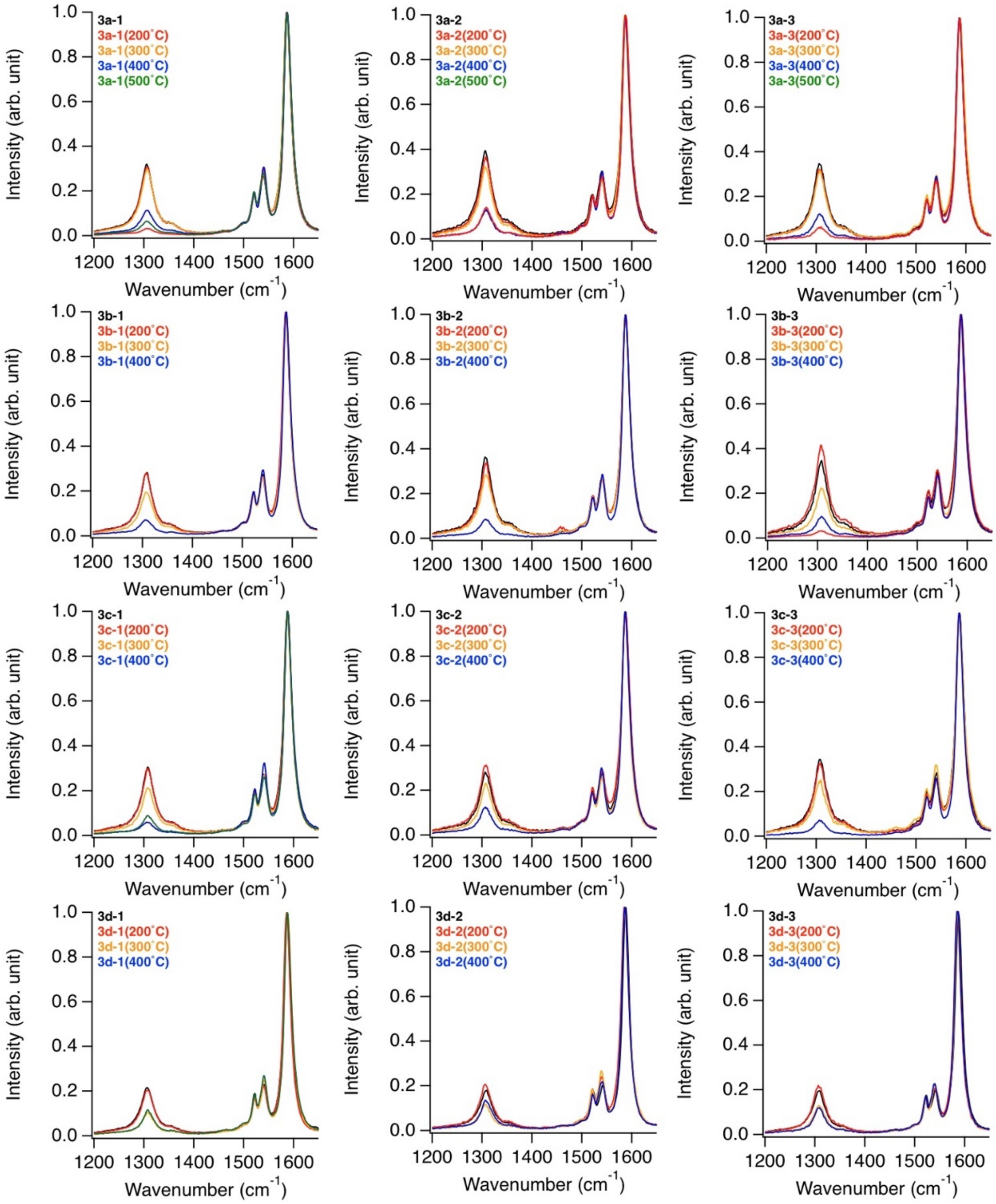

Figure S3. Raman spectra (561 nm excitation) of functionalized SWNTs (**3a-3d**) before and after thermal treatment.

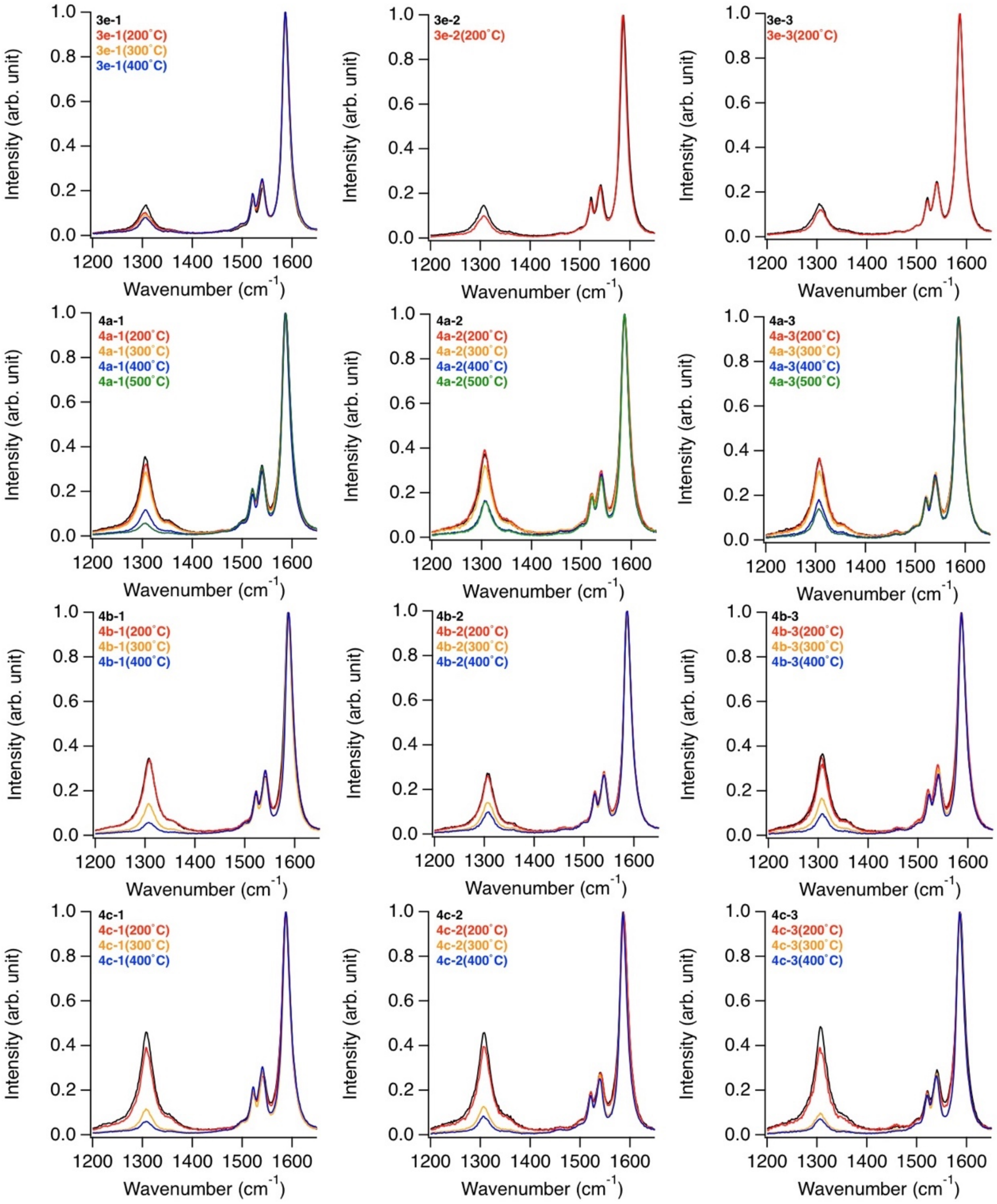

Figure S4. Raman spectra (561 nm excitation) of functionalized SWNTs (**3e**, **4a-4c**) before and after thermal treatment.

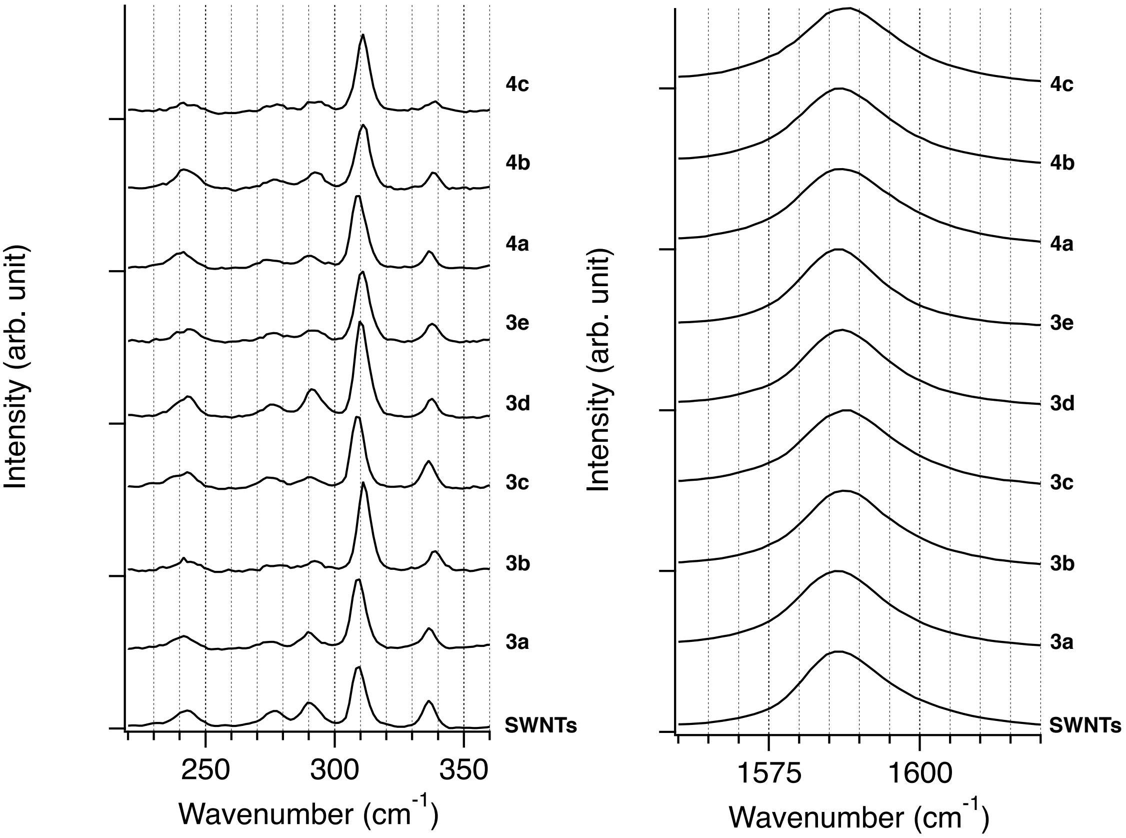

Figure S5. Raman spectra (561 nm excitation) of functionalized SWNTs (**SWNTs**, **3a-3e**, and **4a-4c**).

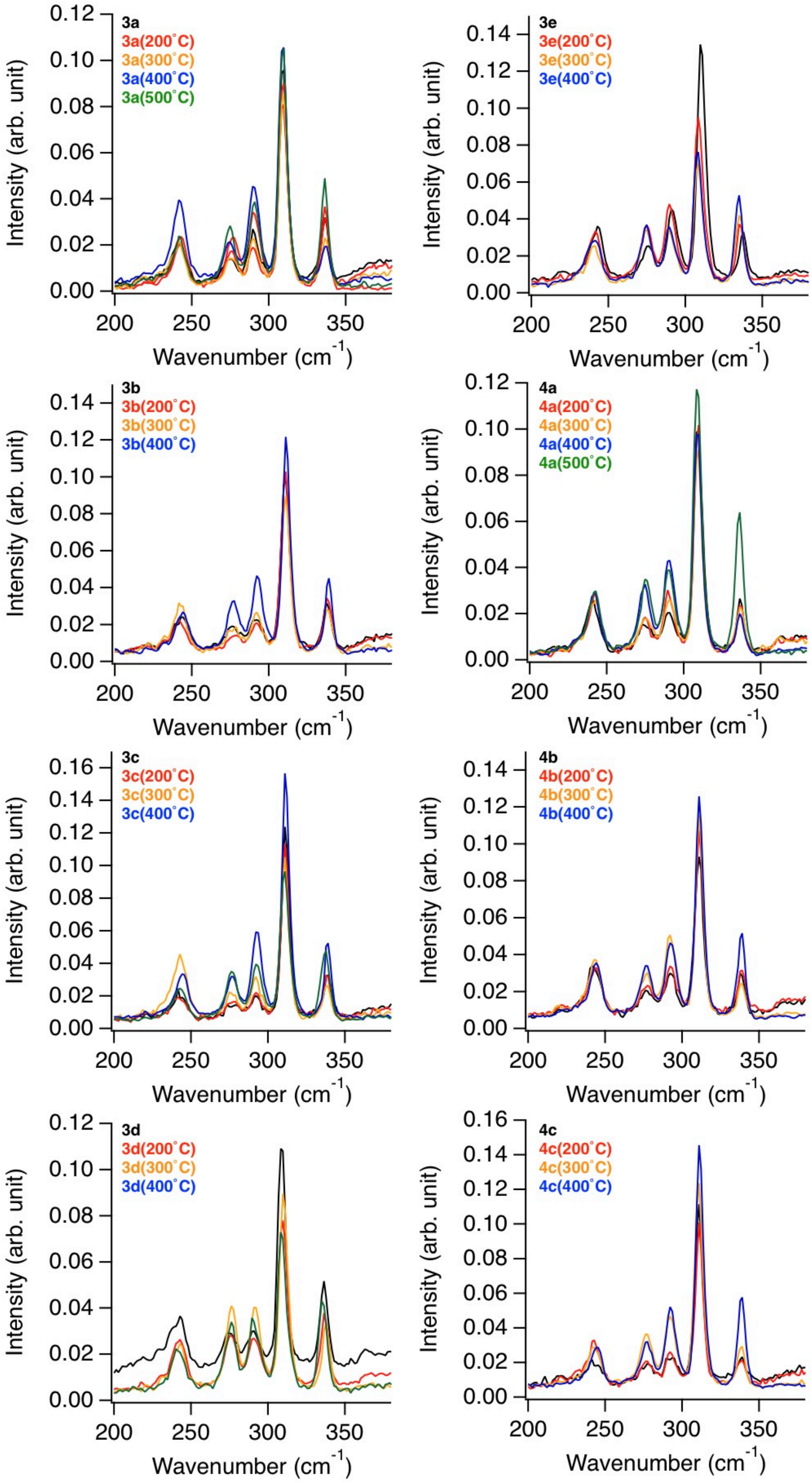

Figure S6. Raman spectra (561 nm excitation) of functionalized SWNTs (**3e**, **4a**-**4c**) before and after thermal treatment.

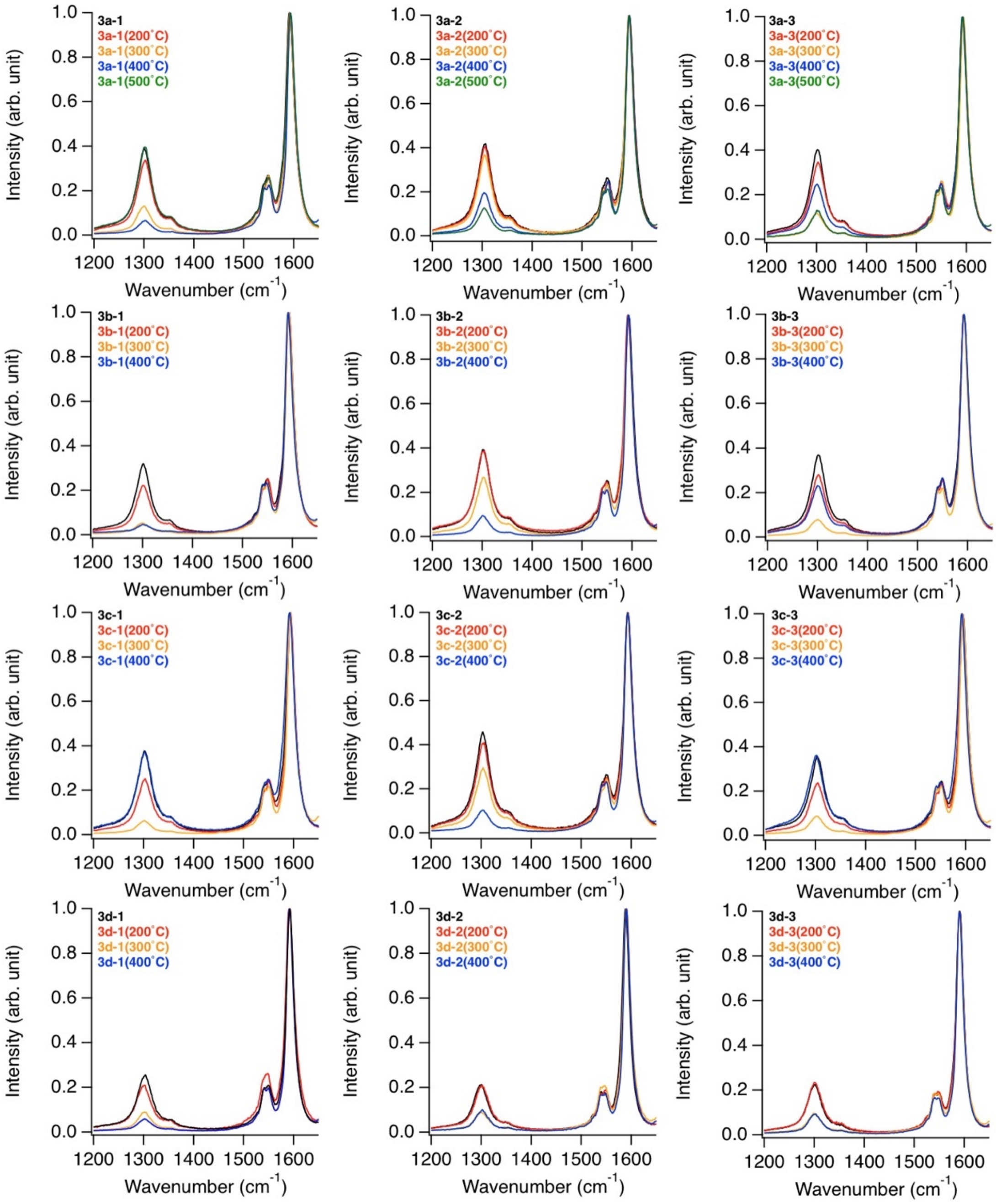

Figure S7. Raman spectra (633 nm excitation) of functionalized SWNTs (**3a-3d**) before and after thermal treatment.

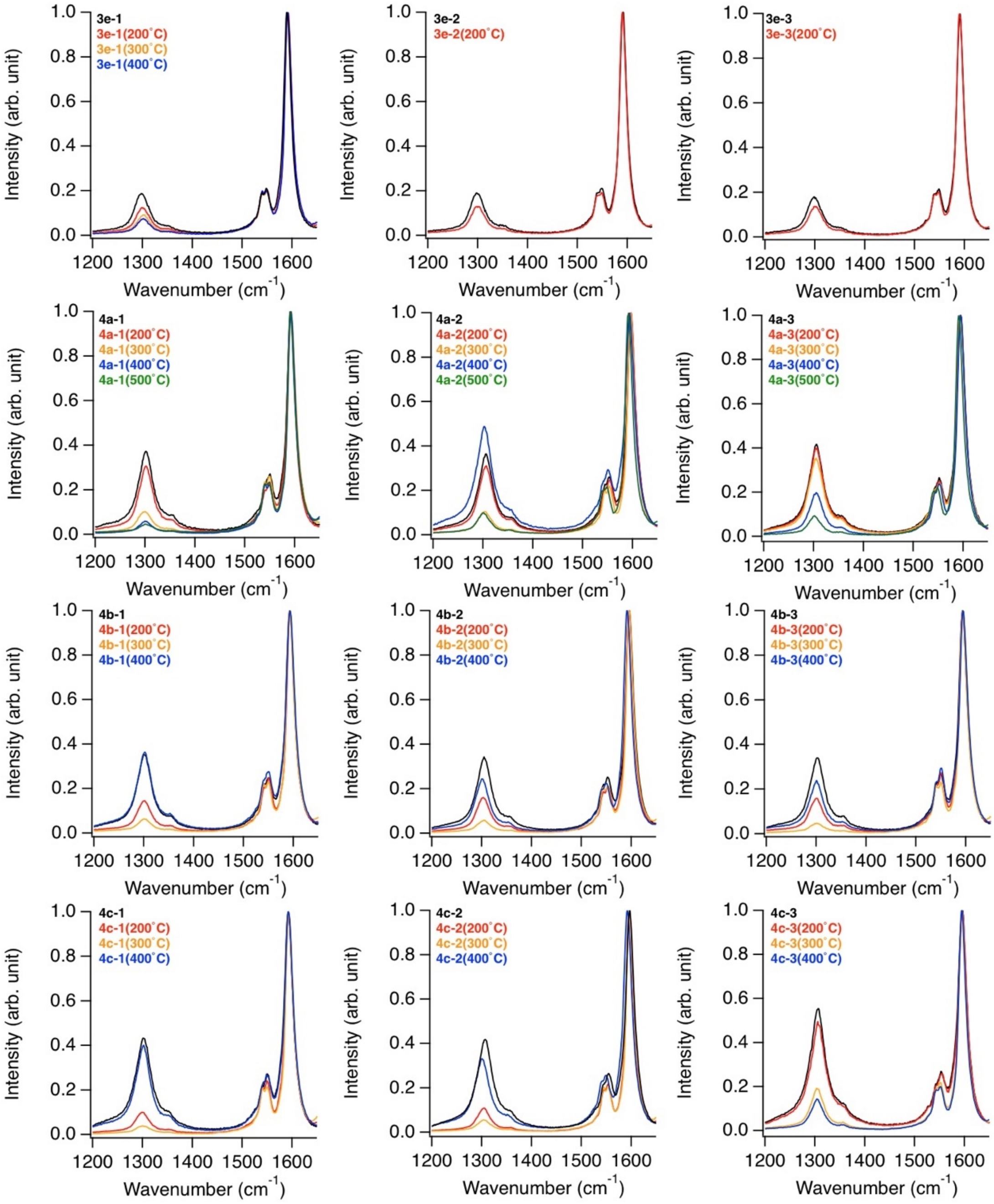

Figure S8. Raman spectra (633 nm excitation) of functionalized SWNTs (**3e**, **4a-4c**) before and after thermal treatment.

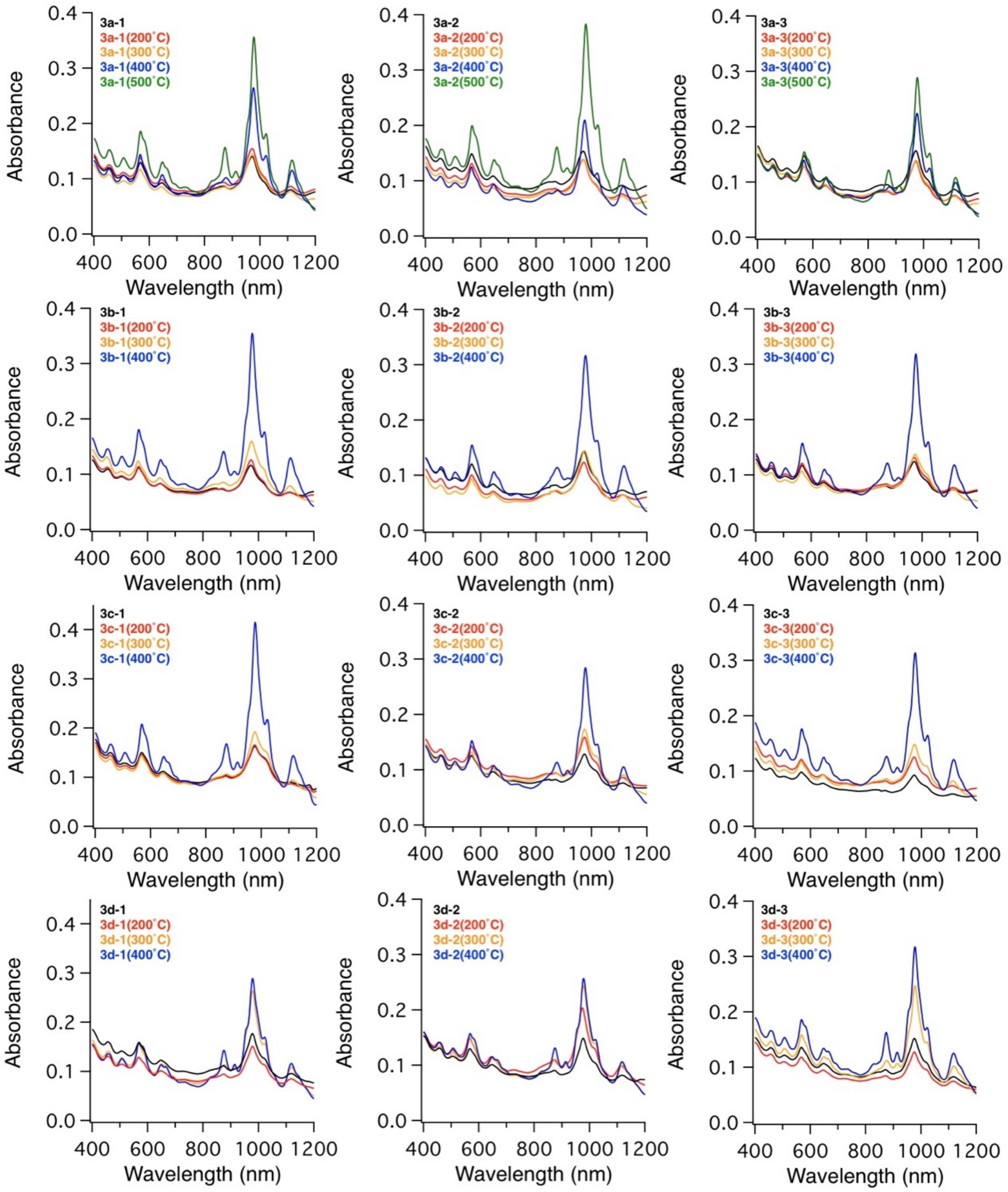

Figure S9. Absorption spectra of functionalized SWNTs (**3a-3d**) before and after thermal treatment in D_2O containing 1wt% SDBS.

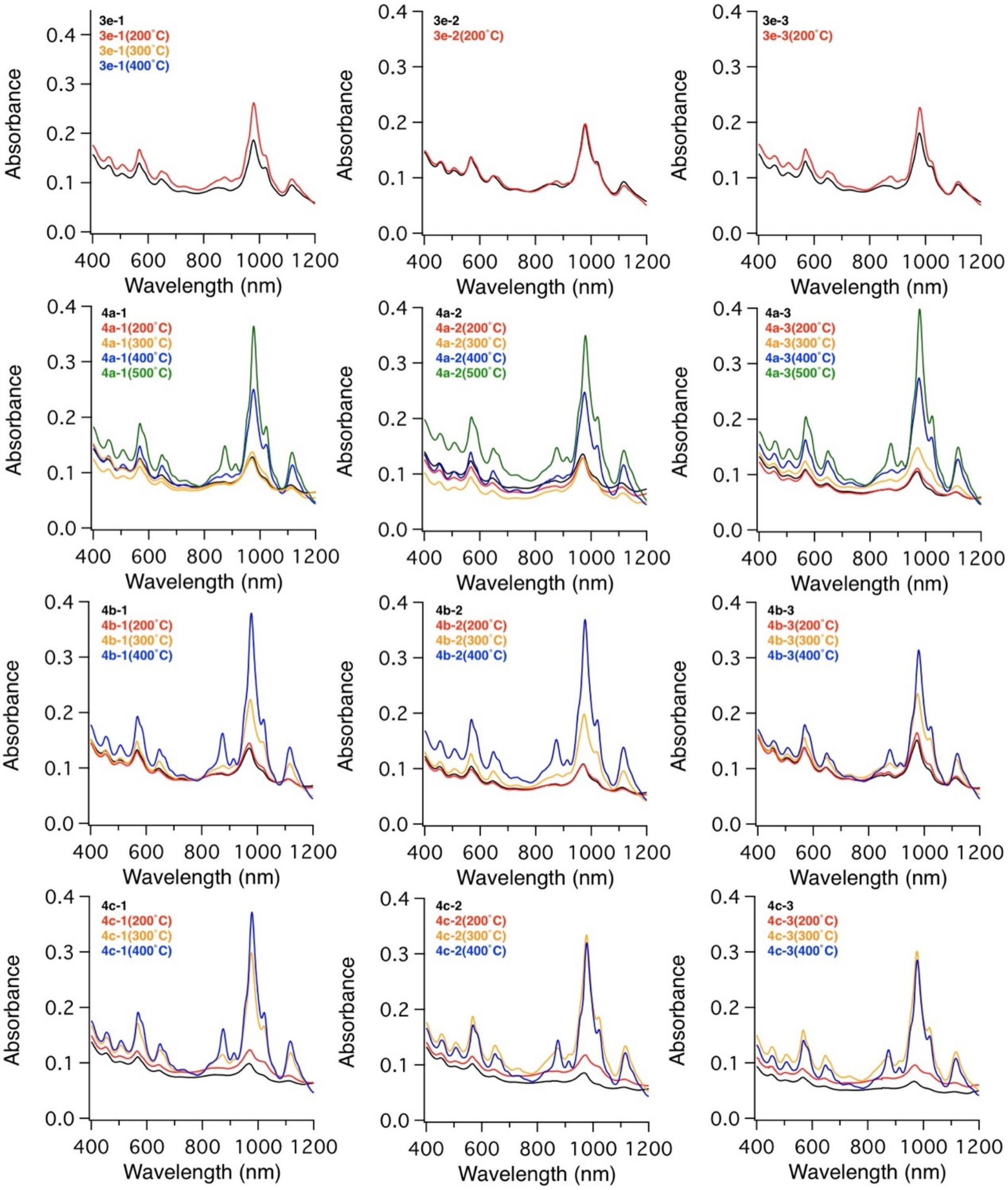

Figure S10. Absorption spectra of functionalized SWNTs (**3e**, **4a-4c**) before and after thermal treatment in D_2O containing 1wt% SDBS.

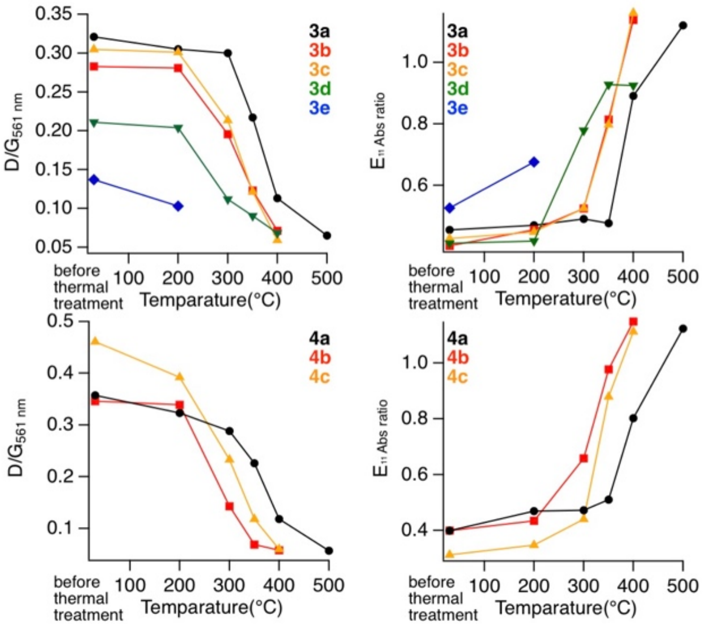

Figure S11. D/G (514.5 nm excitation) and relative E_{11} absorption peak intensity of **3a-e** and **4a-c** as a function of temperature of the thermal treatment.

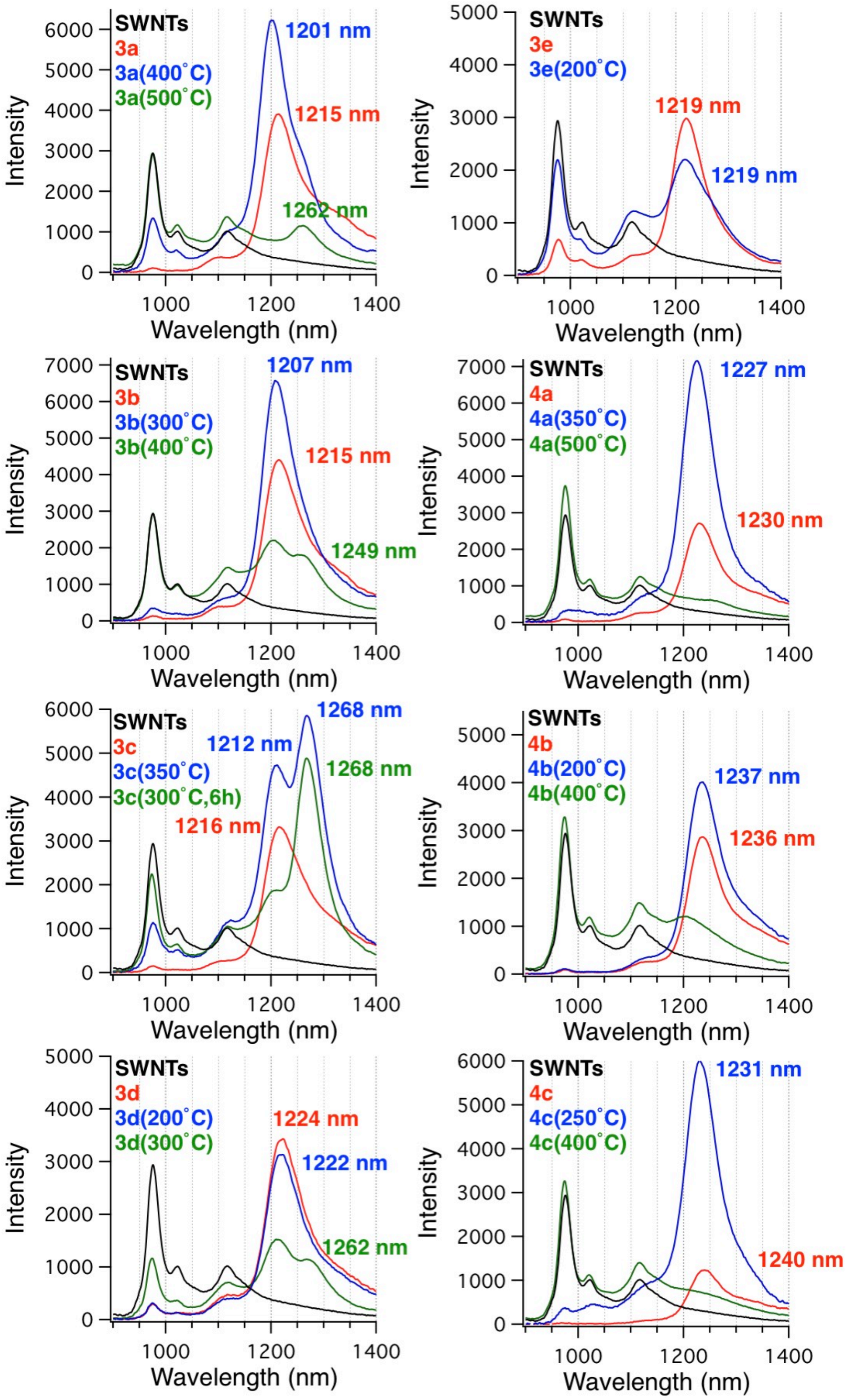

Figure S12. PL spectra (567 nm excitation) of functionalized SWNTs (**3a-3e, 4a-4c**) before and after thermal treatment in D_2O containing 1wt% SDBS.

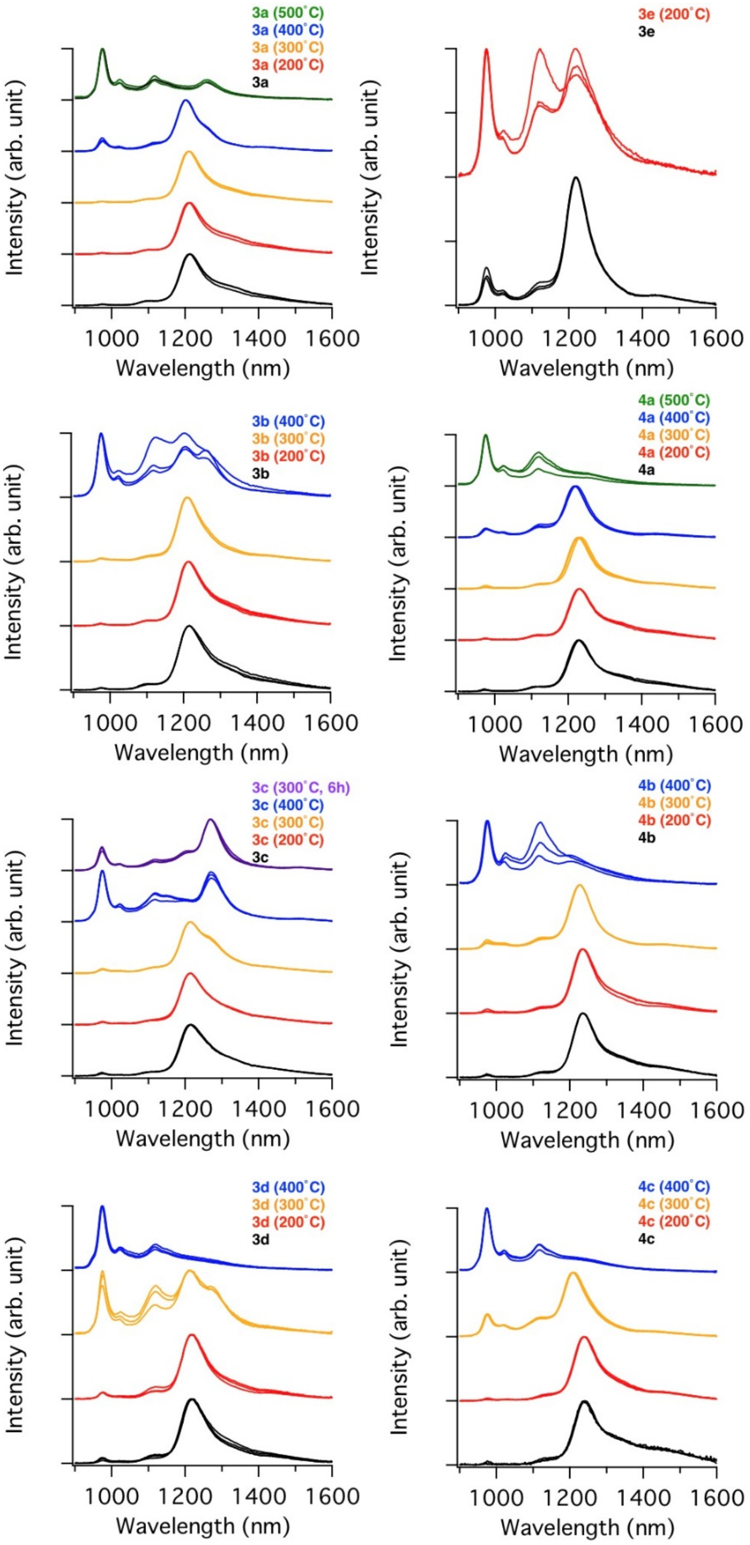

Figure S13. PL spectra of functionalized SWNTs (**3a-3e, 4a-4c**) before and after thermal treatment in D_2O containing 1wt% SDBS (567 nm excitation). These spectra show reproducibility for three times.

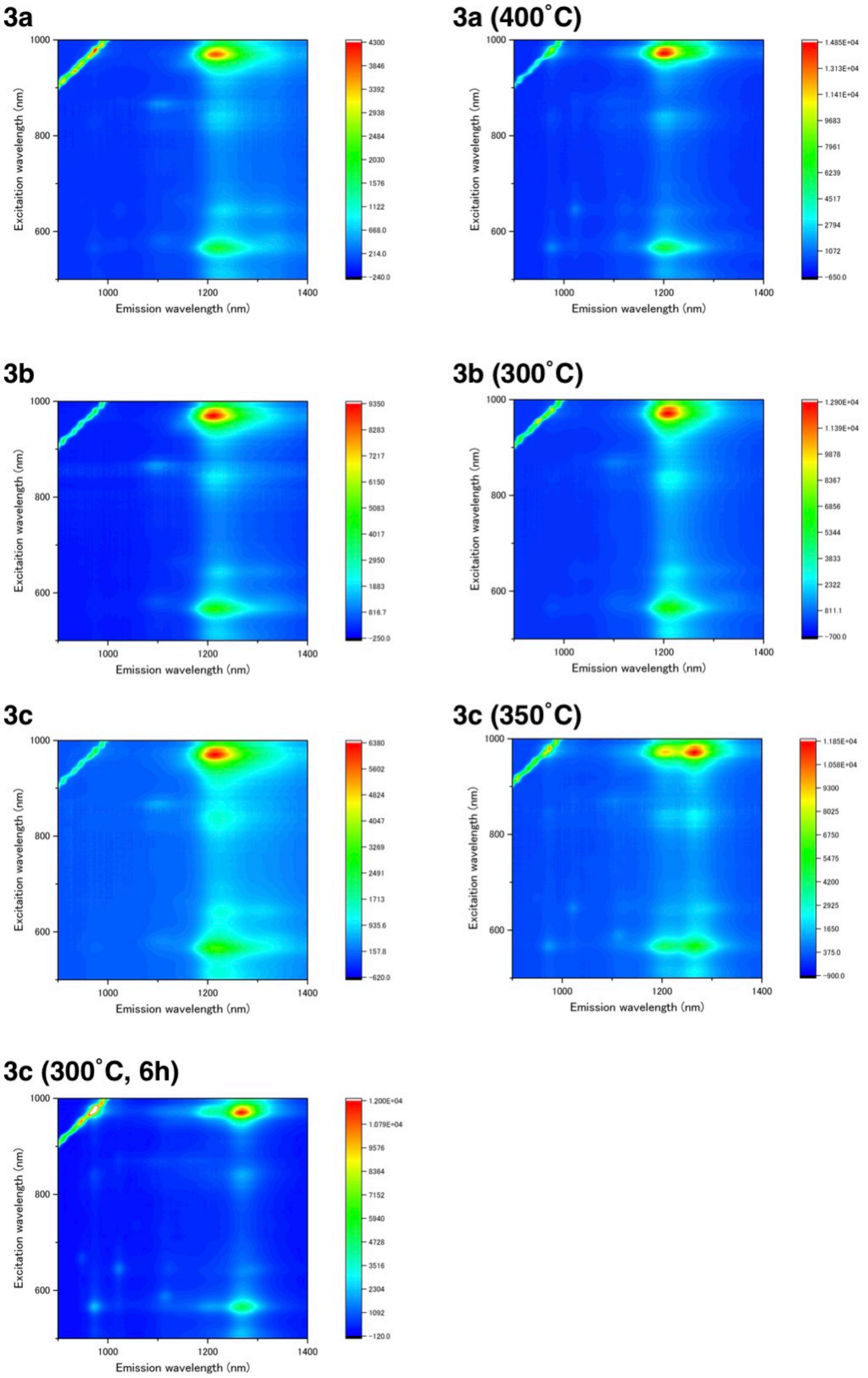

Figure S14. Contour plots of PL intensity versus excitation and emission wavelengths of **3a-3c**.

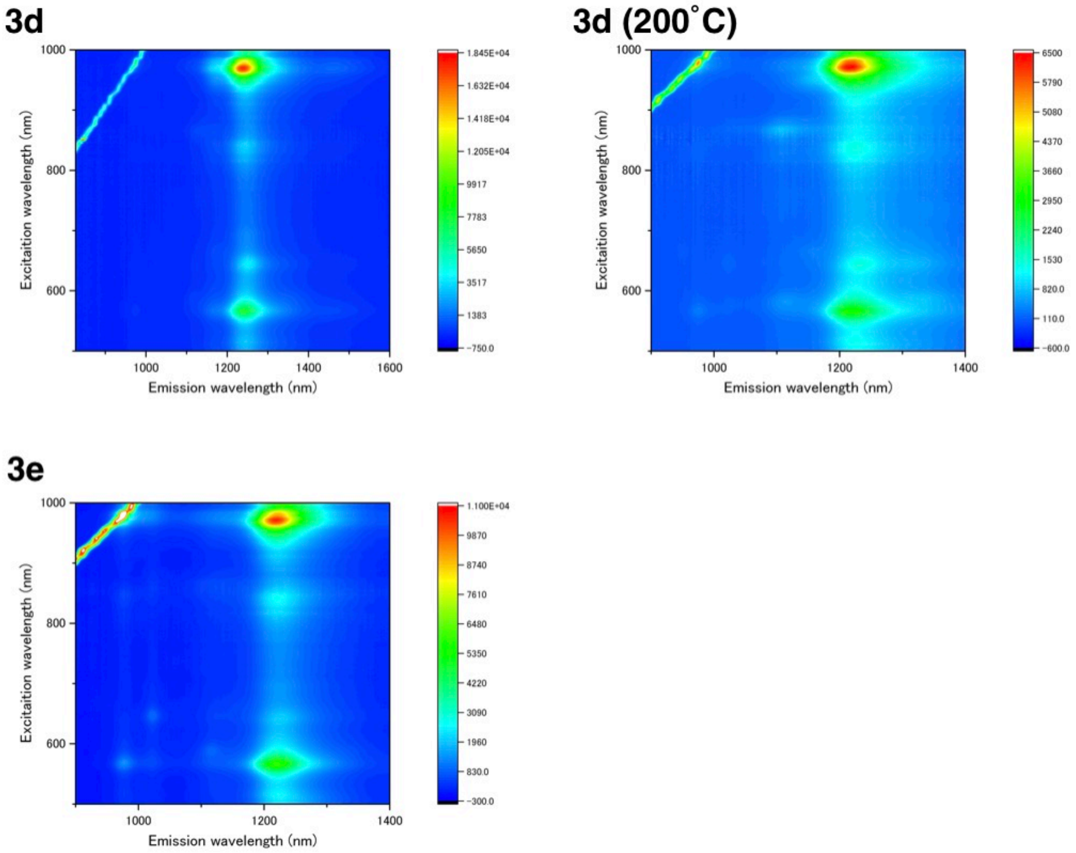

Figure S15. Contour plots of PL intensity versus excitation and emission wavelengths of **3d-3e**.

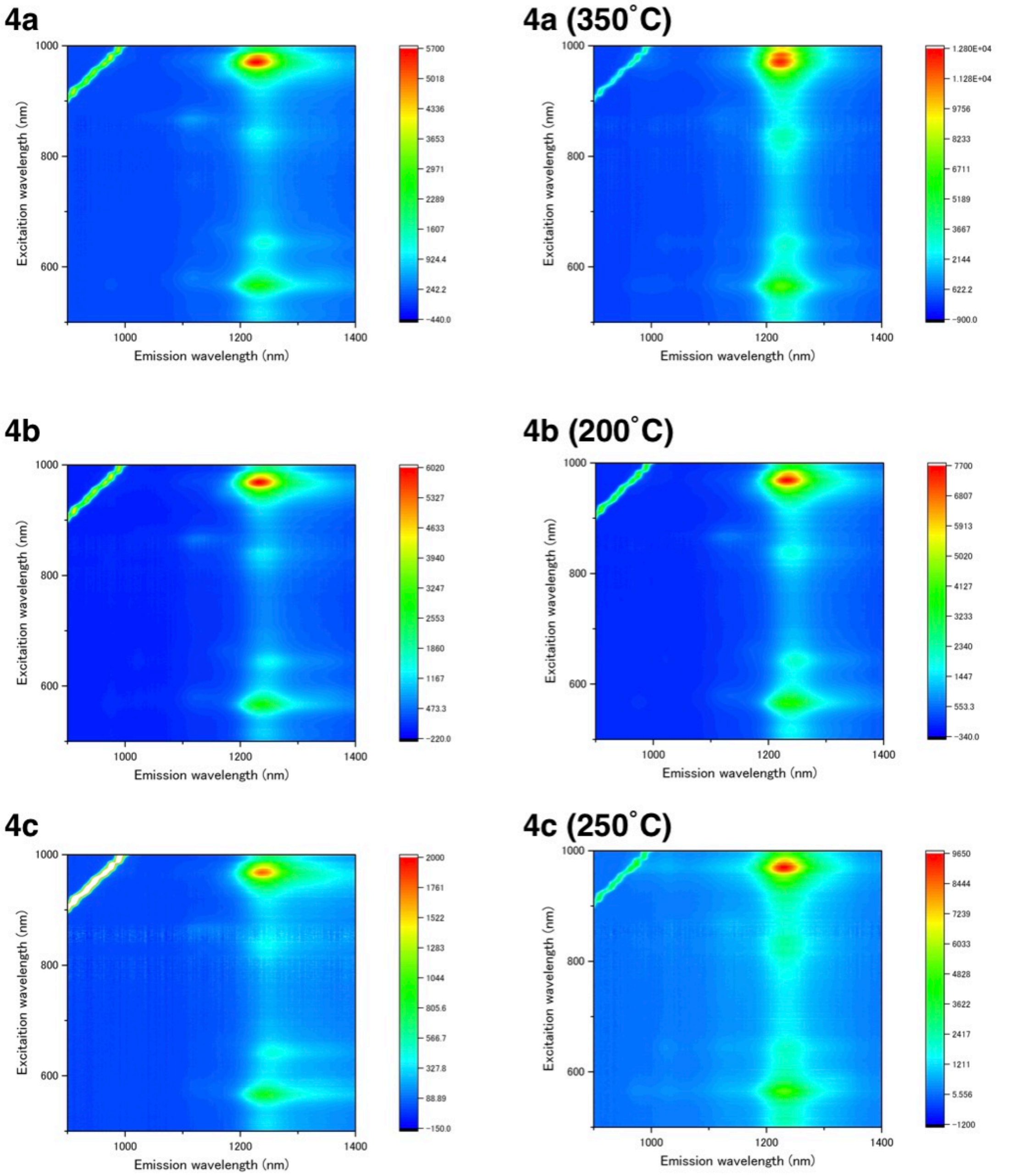

Figure S16. Contour plots of PL intensity versus excitation and emission wavelengths of **4a-4c**.

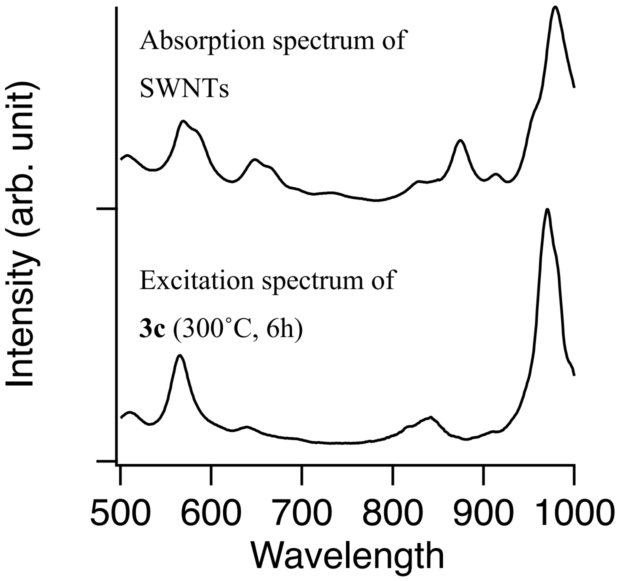

Figure S17. Absorption spectrum of SWNTs and excitation spectra (1268 nm) of **3c** (300˚C, 6h).

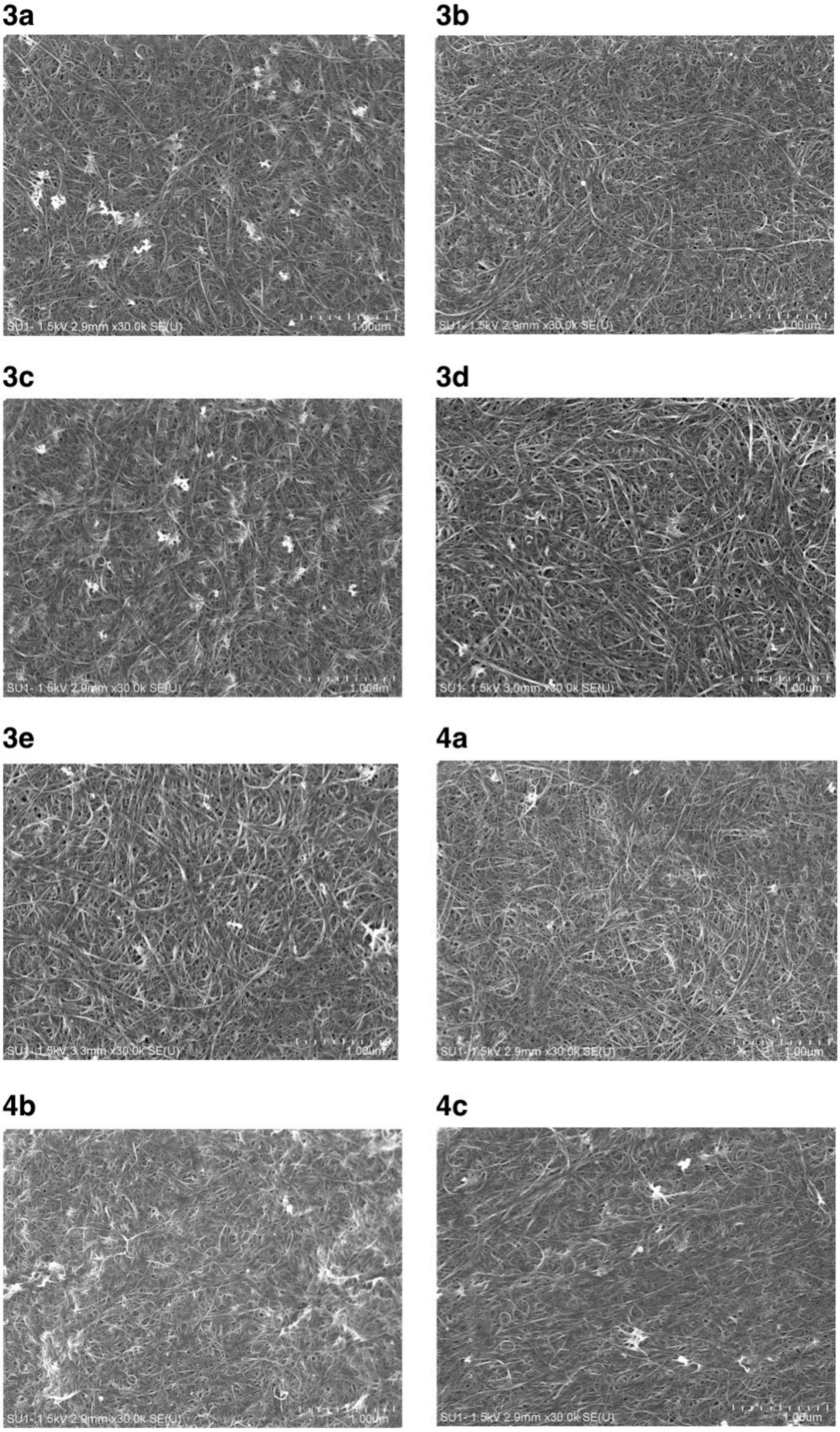

Figure S18. SEM images of functionalized SWNTs.

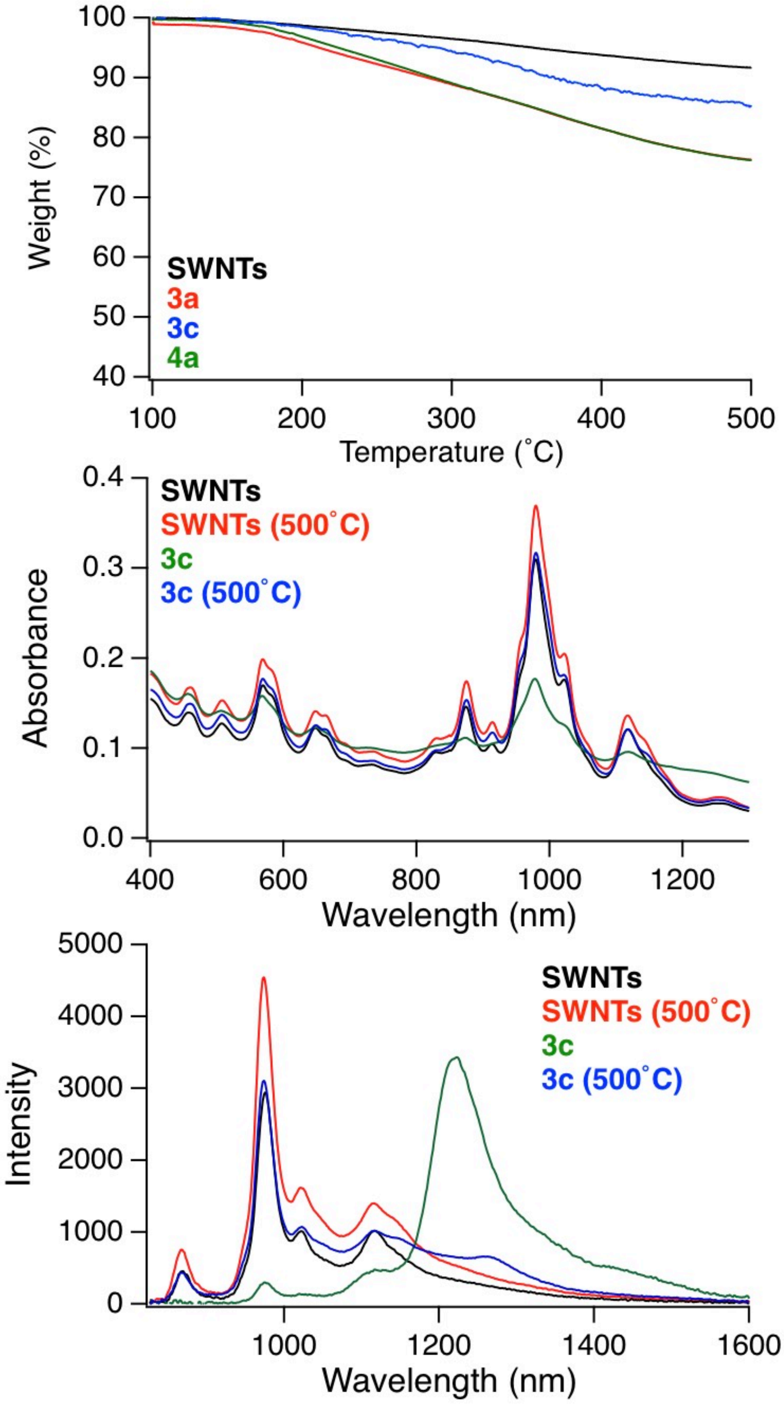

Figure S19. TG curve, absorption, and PL spectra of SWNTs and functionalized SWNTs. Heating rate of 10°C/min. Nitrogen flow rate of 50 mL/min. Weight% at 500˚C; SWNTs 92.0%. **3a** 76.3%[1]. **3c** 85.4%. **4a** 76.2%[1]. Absorption and PL spectra (567 nm excitation of **3c**.)

1: *RSC Adv*. 2019, **9**, 13998.

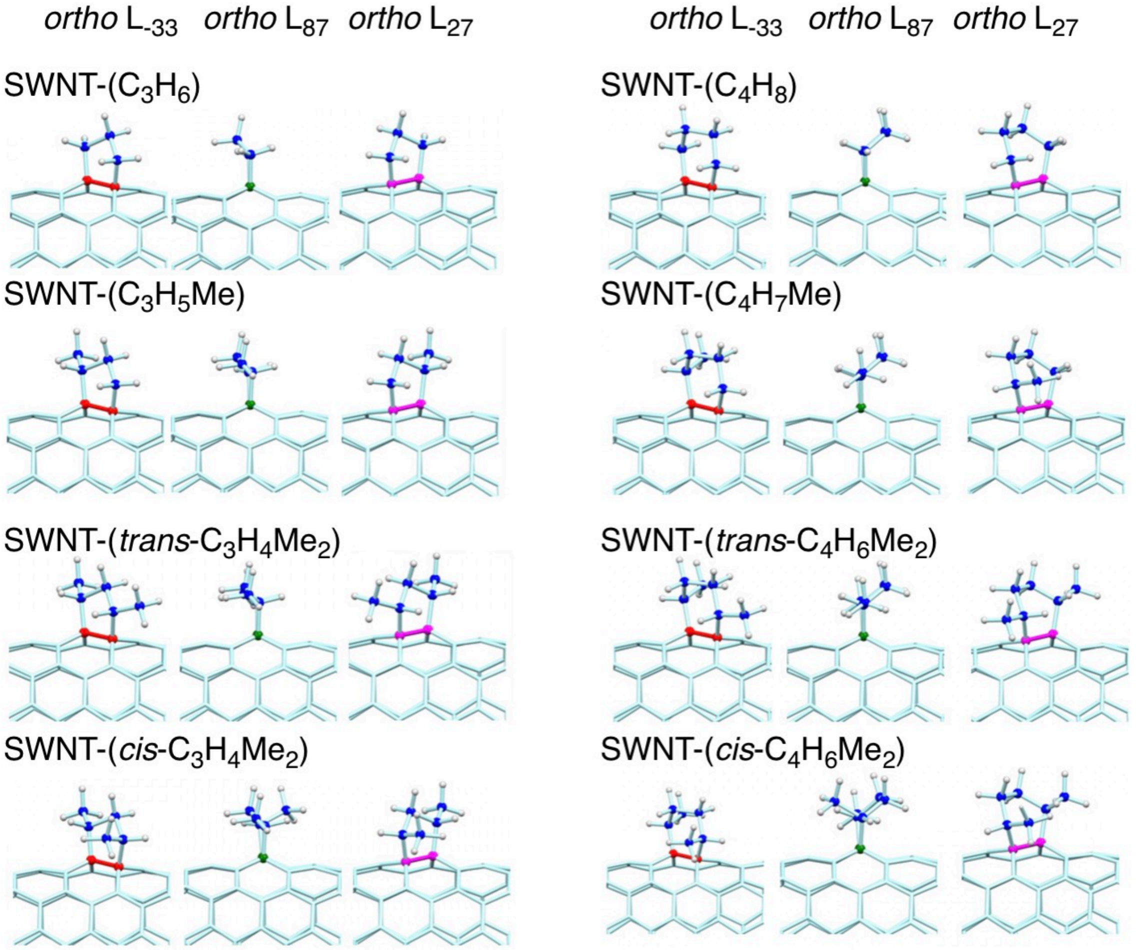

Figure S20. Partial view of the optimized structures of functionalized (6,5) SWNTs by B3LYP/6-31G*.

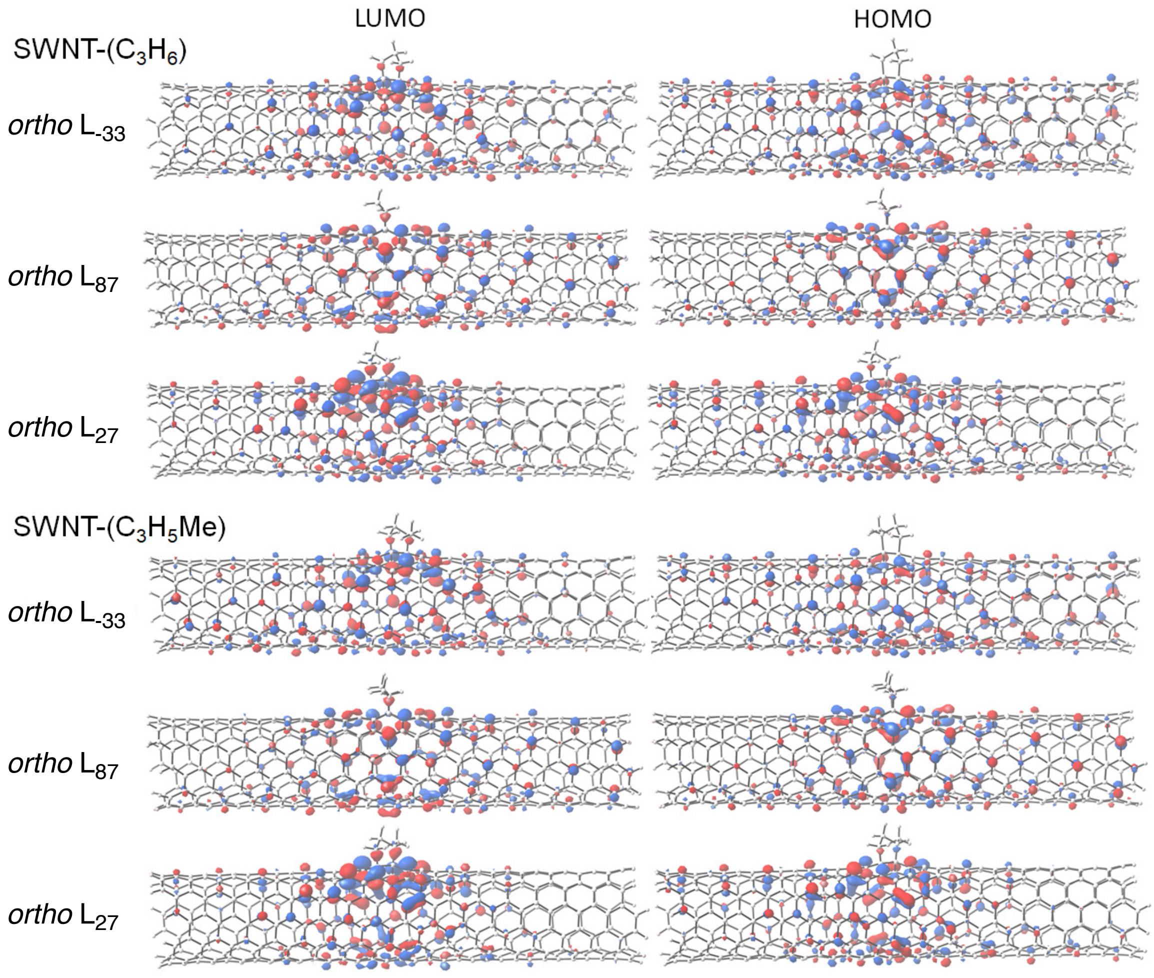

Figure S21. Frontier molecular orbital diagrams of ortho adducts for SWNT-(C_3H_6) and SWNT-(C_3H_5Me) (B3LYP/6-31G*, isovalue=0.02) using 1-unit cell.

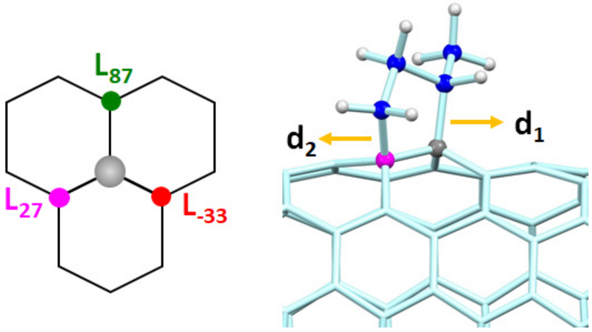

Figure S22 Representation of d_1 and d_2: d_1 stands for the separation between the substituents and the central carbon atom of SWNT (colored in grey), and d_2 represents the distance between the substituents and the other carbon atoms of SWNT (colored in magenta, red and green). The structure of SWNT-C_3H_5Me (*ortho* L_{27}) is shown in right as an example.

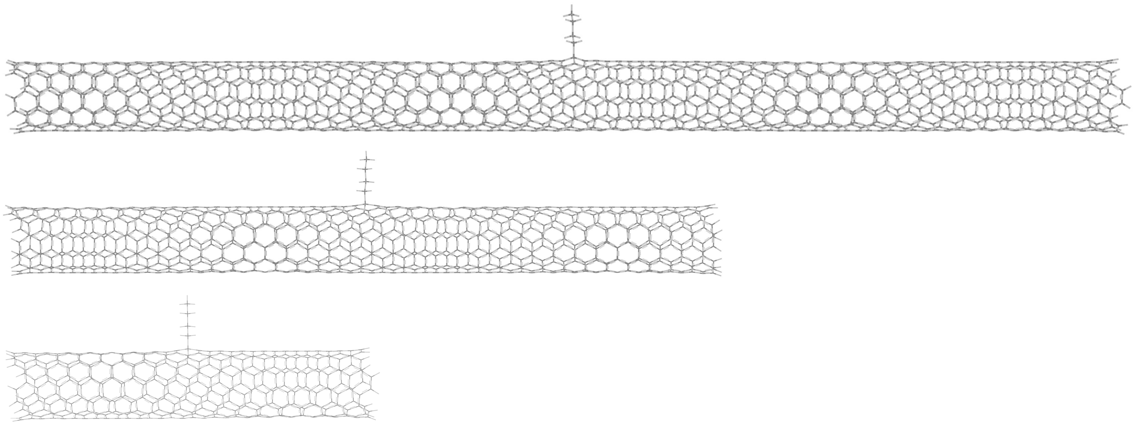

Figure S23. Optimized structure of *n*-butyl (6,5) SWNT radical (*ortho* L_{87}) using UB3LYP/3-21G using 1-, 2-, and 3-unit cells.

There is another possibility of the formation of rearranged isomers via hydrogen atom abstraction (Figure S21). The calculation of the model compounds of the rearrangement isomers via hydrogen atom abstraction for each addition position showed that the absorption peaks were observed at a longer wavelength than that before the rearrangement (Table S5). However, the possibility of the rearrangement via hydrogen atom abstraction is considered to be low because the calculated absorption wavelengths of the rearranged isomer is shorter than that of the model compounds of SWNT-(C_4H_8) when the addition position is the same.

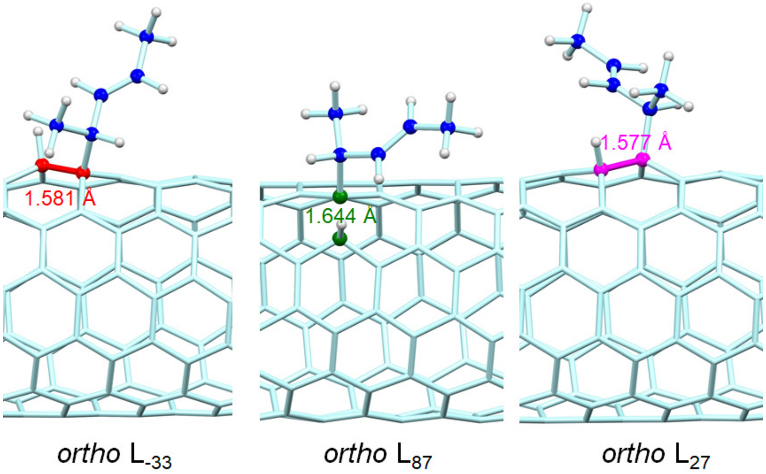

Figure S24. The optimized partial structures of H-SWNT-CH(CH_3)CH=CHCH$_3$ after the rearrangement of SWNT-($C_3H_4Me_2$).

Table S1. D/G, relative E_{11} absorption peak intensity, and PL wavelength of functionalized SWNTs.

	D/G$_{514.5nm}$	D/G$_{561nm}$	D/G$_{633nm}$	relative E_{11} absorption peak intensity
SWNTs	0.13	0.03	0.07	1.00
3a	0.44	0.32	0.40	0.45
3a(200°C)	0.46	0.31	0.39	0.47
3a(300°C)	0.45	0.30	0.34	0.49
3a(400°C)	0.22	0.11	0.13	0.89
3a(500°C)	0.11	0.06	0.07	1.12
3b	0.40	0.28	0.34	0.40
3b(200°C)	0.38	0.28	0.32	0.45
3b(300°C)	0.36	0.20	0.22	0.52
3b(400°C)	0.11	0.07	0.05	1.14
3c	0.41	0.31	0.39	0.43
3c(200°C)	0.44	0.30	0.38	0.45
3c(300°C)	0.39	0.21	0.25	0.52
3c(400°C)	0.11	0.06	0.06	1.16
3d	0.34	0.21	0.26	0.41
3d(200°C)	0.32	0.20	0.21	0.42
3d(300°C)	0.17	0.11	0.09	0.78
3d(400°C)	0.14	0.07	0.06	0.93
3e	0.23	0.14	0.18	0.53
3e(200°C)	0.19	0.10	0.12	0.68
4a	0.46	0.36	0.35	0.40
4a(200°C)	0.48	0.32	0.37	0.47
4a(300°C)	0.45	0.29	0.31	0.47
4a(400°C)	0.19	0.12	0.10	0.80
4a(500°C)	0.11	0.06	0.06	1.12
4b	0.47	0.35	0.40	0.40
4b(200°C)	0.47	0.34	0.34	0.43
4b(300°C)	0.28	0.14	0.16	0.66
4b(400°C)	0.10	0.06	0.05	1.15
4c	0.63	0.46	0.52	0.31
4c(200°C)	0.59	0.39	0.43	0.35
4c(300°C)	0.16	0.12	0.10	0.88
4c(400°C)	0.09	0.06	0.04	1.11

Table S2. Absorption and emission energies of *ortho* adducts for SWNT-C_3H_6 calculated by CAM-B3LYP/STO-3G using 3-unit cells.

SWNTs	absorption		emission		
	eV	nm	eV	nm	corrected $E_{11}*(\infty)$
ortho L_{-33}	1.91	648	1.74	711	1.13
ortho L_{87}	1.84	674	1.66	748	1.08
ortho L_{27}	1.62	767	1.41	879	0.93
pristine	1.97	628	1.95	634	/

Table S3. Relative energies (in kcal/mol) of functionalized (6,5) SWNTs calculated by DFT with B3LYP/6-31G* using 1-unit cell and calculated absorption wavelengths of functionalizaed (6,5) SWNTs using TD-DFT with B3LYP/3-21G using 1-unit cell.

		ortho L_{-33}	*ortho* L_{87}	*ortho* L_{27}
SWNT-(C_3H_6)[26]	relative energy	0	4.6	1.9
	absorption wavelength	880	920	1099
SWNT-(C_3H_5Me)	relative energy	0	3.7	2.2
	absorption wavelength	880	920	1099
SWNT-(*cis*-$C_3H_4Me_2$)	relative energy	0	1.7	2.9
	absorption wavelength	881	920	1102
SWNT-(*trans*-$C_3H_4Me_2$)	relative energy	0	4.7	2.0
	absorption wavelength	883	922	1104
SWNT-(C_4H_8) [26]	relative energy	0	7.9	3.7
	absorption wavelength	885	934	1120
SWNT-(C_4H_7Me)	relative energy	0	3.8	2.7
	absorption wavelength	888	934	1125
SWNT-(*cis*-$C_4H_6Me_2$)	relative energy	1.5	0	6.4
	absorption wavelength	891	935	1127
SWNT-(*trans*-$C_4H_6Me_2$)	relative energy	0.6	5.1	4.8
	absorption wavelength	893	938	1130

Table S4. Bond length (d_1 and d_2, in Å, see Figure S19) of the formed C-C bonds between SWNT and substituents that are obtained at the level of B3LYP/6-31G* using 1-unit cell. (Bond length of the formed C-C bond with the carbon atom attached the methyl group in SWNT-(C_3H_5Me) and (SWNT-C_4H_7Me) are in bold.)

addition site	d_1	d_2	d_1	d_2
	SWNT-(C_3H_6)		SWNT-(C_4H_8)	
ortho L_{-33}	1.568	1.598	1.58	1.579
ortho L_{87}	1.586	1.589	1.584	1.583
ortho L_{27}	1.597	1.567	1.57	1.583
	SWNT-(C_3H_5Me)		SWNT-(C_4H_7Me)	
ortho L_{-33}	1.567	**1.622**	**1.609**	1.581
ortho L_{87}	**1.605**	1.59	**1.607**	1.581
ortho L_{27}	**1.621**	1.566	**1.592**	1.582
	SWNT-(*cis*-$C_3H_4Me_2$)		SWNT-(*cis*-$C_4H_6Me_2$)	
ortho L_{-33}	1.591	1.623	1.613	1.613
ortho L_{87}	1.605	1.609	1.606	1.604
ortho L_{27}	1.616	1.591	1.594	1.619

Table S5. Spin density of *n*-butyl (6,5) SWNT radical (*ortho* L_{87}) using UB3LYP/3-21G using 1-, 2-, and 3-unit cells.

addition site	1 unit	2 unit	3 unit
ortho L_{-33}	0.2228	0.2217	0.2215
ortho L_{87}	0.2257	0.2280	0.2281
ortho L_{27}	0.1569	0.1589	0.1590
para L_{-33}	0.1296	0.1317	0.1318
para L_{87}	0.1707	0.1701	0.1701
para L_{27}	0.1948	0.1960	0.1961

Table S6. Relative energies (in kcal/mol) of H-SWNT-CH(CH$_3$)CH=CHCH$_3$ after the rearrangement of SWNT-(C$_3$H$_4$Me$_2$) calculated by DFT with B3LYP/6-31G* using 1-unit cell (with respect to the most stable isomer of SWNT-(C$_3$H$_4$Me$_2$) in Table 1). Calculated absorption wavelengths of H-SWNT-CH(CH$_3$)CH=CHCH$_3$ using TD-DFT with B3LYP/3-21G using 1-unit cell.

addition site	ΔE	E_{abs}	*f*
ortho L_{-33}	14.9	883	0.5215
ortho L_{87}	21.1	926	0.7139
ortho L_{27}	16	1109	0.9469

Table S7. Total energies (in a.u.) of functionalized (6,5) SWNTs calculated by DFT with B3LYP/6-31G* using 1-unit cell.

addition site	SWNT-(C$_3$H$_6$)	SWNT-(C$_3$H$_5$Me)	SWNT-(C$_3$H$_4$Me$_2$)		
			cis	*trans*	rearrangement
ortho L_{-33}	-14003.7374286	-14043.0495609	-14082.3593664	-14082.3593053	-14082.3355418
ortho L_{87}	-14003.7301413	-14043.0436296	-14082.3566619	-14082.3518556	-14082.3257437
ortho L_{27}	-14003.7343939	-14043.0460769	-14082.3546996	-14082.3561993	-14082.3339357

addition site	SWNT-(C$_4$H$_8$)	SWNT-(C$_4$H$_7$Me)	SWNT-(C$_4$H$_6$Me$_2$)	
			cis	*trans*
ortho L_{-33}	-14043.0454506	-14082.3497609	-14121.6514859	-14121.6529239
ortho L_{87}	-14043.0329049	-14082.3436381	-14121.6539480	-14121.6458685
ortho L_{27}	-14043.0395043	-14082.3454590	-14121.6437019	-14121.6462722

Table S8. Relative energies of functionalized SWNTs calculated by B3LYP, M06-2X, and ωB97XD with the 6-31G* basis sets.

		B3LYP/6-31G*	M06-2X/6-31G*	ωB97XD/6-31G*
SWNT-(C$_3$H$_6$)	*ortho* L_{-33}	0	0	0
	ortho L_{87}	4.6	5.4	5.4
	ortho L_{27}	1.9	2.5	2.9
SWNT-(C$_3$H$_5$Me)	*ortho* L_{-33}	0	0	0
	ortho L_{87}	3.7	4.5	4.6
	ortho L_{27}	2.2	2.8	3.2
SWNT-(*cis*-C$_3$H$_4$Me$_2$)	*ortho* L_{-33}	0	0	0
	ortho L_{87}	1.7	2.8	2.8
	ortho L_{27}	2.9	3.5	3.9